



**HAL**  
open science

## On the deactivation of the dopant and electronic structure in reactively sputtered transparent Al-doped ZnO thin films

David Horwat, Maud Jullien, Fabien Capon, Jean-François Pierson, Joakim Andersson, José Luis Endrino

► **To cite this version:**

David Horwat, Maud Jullien, Fabien Capon, Jean-François Pierson, Joakim Andersson, et al.. On the deactivation of the dopant and electronic structure in reactively sputtered transparent Al-doped ZnO thin films. *Journal of Physics D: Applied Physics*, 2010, 43 (13), pp.132003. 10.1088/0022-3727/43/13/132003 . hal-00569420

**HAL Id: hal-00569420**

**<https://hal.science/hal-00569420>**

Submitted on 25 Feb 2011

**HAL** is a multi-disciplinary open access archive for the deposit and dissemination of scientific research documents, whether they are published or not. The documents may come from teaching and research institutions in France or abroad, or from public or private research centers.

L'archive ouverte pluridisciplinaire **HAL**, est destinée au dépôt et à la diffusion de documents scientifiques de niveau recherche, publiés ou non, émanant des établissements d'enseignement et de recherche français ou étrangers, des laboratoires publics ou privés.

## On the deactivation of dopant and electronic structure in reactively sputtered transparent Al-doped ZnO thin films

David Horwat<sup>1,4</sup>, Maud Jullien<sup>1</sup>, Fabien Capon<sup>1</sup>, Jean-François Pierson<sup>1</sup>, Joakim Andersson<sup>2</sup> and José Luis Endrino<sup>3</sup>

<sup>1</sup>Institut Jean Lamour, Département CP2S, UMR 7198 CNRS-Nancy-Université-UPV-Metz, Ecole des Mines de Nancy, Parc de Saurupt, CS14234, 54042 Nancy, France.

<sup>2</sup>The Angstrom Laboratory, Uppsala University, Box 530, SE-75121 Uppsala, Sweden

<sup>3</sup>Instituto de Ciencia de Materiales de Madrid, C.S.I.C., Madrid 28049, Spain

<sup>4</sup>Author to whom the correspondence should be addressed; electronic mail:

david.horwat@mines.inpl-nancy.fr

### Abstract

We report on a possible origin of electrical heterogeneities in 4 at% Al doped ZnO (AZO) reactively sputtered films. It is found through Zn  $L_3$  and Al  $K$  edge X-ray absorption near edge structure (XANES) that a fraction of the Al dopant is deactivated by its positioning in octahedral conformation with oxygen. This fraction as well as the conductivity, optical bandgap and  $c$ -axis parameter of ZnO wurtzite are all found to depend on the sample position during deposition. The present results suggest the formation of a metastable  $\text{Al}_2\text{O}_3(\text{ZnO})_m$  homologous phase that degrades the electrical conductivity.

Transparent conducting oxides (TCOs) characterized by both high transparency in the visible range and high electrical conductivity are key materials for devices such

as transparent thin film transistors [1], solar cells [2, 3] and UV light emitting diodes [4]. Among materials with n-type conductivity, zinc oxide with a Wurtzite structure (w-ZnO, P6<sub>3</sub>mc space group) doped with trivalent metal ions [5] (Al<sup>3+</sup>, Ga<sup>3+</sup>, In<sup>3+</sup>) represents a promising alternative to indium-doped tin oxide (ITO) and fluorine-doped tin oxide (SnO<sub>2</sub>:F). Interest in n-type ZnO has intensified for several reasons: the greater availability of zinc and aluminum compared to tin and indium; the high transparency of n-type ZnO; and the electronic conductivity of n-type ZnO, which is presently equivalent to ITO but has potential for further improvement [6]. A few studies on Al doped ZnO (AZO) deposition have considered the issue of lateral heterogeneity of material properties, which is of prime importance in practical device production. In various magnetron sputtering (MS) experimental configurations [7, 8], the resistivity of AZO films was found to be highly sensitive to the position of the samples with respect to the sputtering target. *Tominaga et al* [8] showed a clear correlation between local drops in conductivity and the flux of energetic oxygen particles drifting from the magnetron plasma loop to the growing film. A subsequent deactivation of the metal dopant by aluminum oxide formation was suggested. Since oxygen sub- and overstoichiometry also strongly affects the conductivity of pure ZnO and AZO [9, 10], it has been difficult to identify the true origin of the lateral heterogeneity of electrical conductivity.

To investigate the origin of the lateral electrical heterogeneity, AZO films were prepared on soda lime glass substrates using reactive magnetron sputtering (MS) of an Al (4 at%)-Zn target. The target-substrate distance was 50 mm and the 2 inches diameter target was positioned off-center relative to the rotating substrate holder to ensure good thickness homogeneity (close to 200 nm). The target was sputtered in D.C. mode in an Ar–16.7 vol% O<sub>2</sub> reactive mixture at 0.3 Pa by dissipating 37 W (0.1

A, 370 V). Samples were positioned at different distances from the target axis, as displayed in the lower inset of Figure 1. Rutherford backscattering spectrometry confirmed that the aluminum content was 4 at%, independent of the positioning of the sample in the reactor. The films were characterized using X-ray diffraction (XRD), UV-visible spectrophotometry, 4 point probe measurement and X-ray absorption near-edge structure (XANES) measurements at the *Al K* and *Zn L<sub>3</sub>* edges. XANES spectra were recorded at the SGM beamline at the Canadian Light Source. Both the surface-sensitive total electron yield (TEY) and the bulk-sensitive fluorescence yield (FLY) were measured simultaneously under quasi-normal excitation and takeoff at 45° from the surface.

Figure 1 shows the transmittance spectra of the AZO films. The optical transmittance exceeds 85% in the visible range. The optical band gap is observed to shift towards higher energies for samples deposited at larger distances from the target axis (position sequence 1-4). The upper inset of Figure 1 is a plot of the electronic conductivity  $\sigma$  versus the measured optical bandgap shift  $\Delta E_g$ . A linear fit to the data is given as

$$\sigma = 156 \times \Delta E_g \quad (1)$$

where  $\Delta E_g$  is the bandgap shift from the value obtained in position 1. Such a shift may result from the Burstein Moss effect [11]. Thus, equation (1) is a strong clue of the dependency of the conductivity to the free carriers (electrons) concentration and possible deactivation of the dopants as the sample position approaches the circumference facing the target axis.

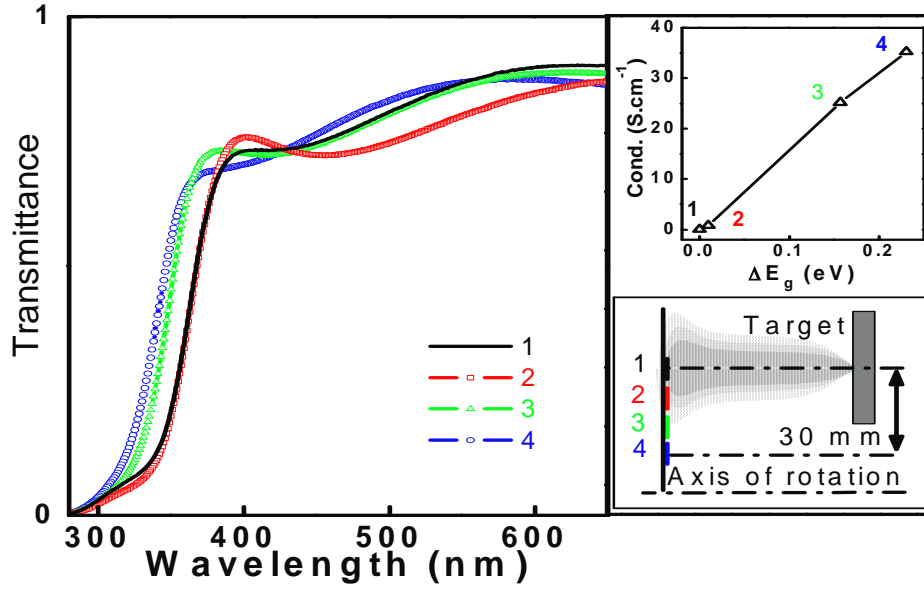


FIG. 1. Optical transmittance spectra of c-axis oriented AZO films deposited on a rotating substrate at circumferences of 0, 10, 20 and 30 mm from the target axis. The lower inset displays a schematic of the experimental configuration. The upper inset displays the dependency between the electronic conductivity and optical band gap shift.

From the magnitude of the shift, the carrier concentration in position 4 can be estimated to approach  $10^{19} \text{ cm}^{-3}$  and the mobility to be very low and close to  $1 \text{ cm}^2/(\text{V}\cdot\text{s})$ . The slight decrease of the oxygen partial pressure during deposition, with all samples maintaining a high film transparency, did not significantly affect the conductivity at position 4 while it improved the conductivity in positions 1-3. This has already been observed for AZO films containing around 1.5 at % Al [7]. Nevertheless, the maximum conductivity was about 40 times higher in agreement with the existence of an optimum dopant concentration. When Al solutes substitute cation sites in ZnO, two kinds of defect equations are usually considered:



Where  $e'$  is a free electron.

and



Substitution according to eq. 2 is predominant in dilute systems while the formation of doubly negatively charged Zn vacancies  $\text{V}_{\text{Zn}}''$  as described in Eq. 3 [12] may impair the doping mechanism and reduce the mobility above a composition threshold. Moreover, the formation of Zn vacancies may be facilitated by the bombardment by oxygen ions [13] which is larger on the magnetron axis [14]. However, a recent study showed that homologous  $\text{Al}_2\text{O}_3(\text{ZnO})_m$  structures similar to those found in ITO compounds could be formed in highly doped AZO films with formation energies lower than those required for Zn vacancies [15]. Such structures can schematically be regarded as nanolaminates of poorly doped ZnO blocks alternating along the  $c$ -axis with  $\text{Al}_2\text{O}_3$ -like monolayers. In the present study the possible formation of homologous  $\text{Al}_2\text{O}_3(\text{ZnO})_m$  structures in reactively sputtered Al-doped ZnO films is investigated using X-ray absorption near edge structure (XANES).

The Zn  $L_3$  edge spectra of samples 1 and 4 are shown in Figure 2(a). According to the dipole-transition selection rule, Zn  $L_3$  edge XANES probes the unoccupied Zn  $s$ - and  $d$ -derived states. Since the Zn  $3d$  orbital is fully occupied, absorption measurements over this edge probe Zn  $4s$  and Zn  $4d$  states. Feature  $A_1$  (~1016 eV) can be ascribed to the Zn  $4s$  derived state, and features  $B_1$  (~1020 eV),  $C_1$  (~1023.5 eV) and  $D_1$  (~1026 eV) to Zn  $4d$  derived states [16]. The density of unoccupied states at the very bottom of the conduction band (feature  $A_1$ ) is largely insensitive to the sample position. On the contrary, features  $B_1$ - $D_1$  are increased for the sample with higher resistivity (sample 1). The overall density of unoccupied states

near the bottom of the conduction band is higher for this sample which is consistent with the Burstein Moss shift of the optical band gap. Moreover, the sharper features in sample 1 indicate a stronger localization of states, in accordance with the increase in resistivity. It can also be stated that surface mechanisms are not dominating since FLY and TEY signals are very similar.

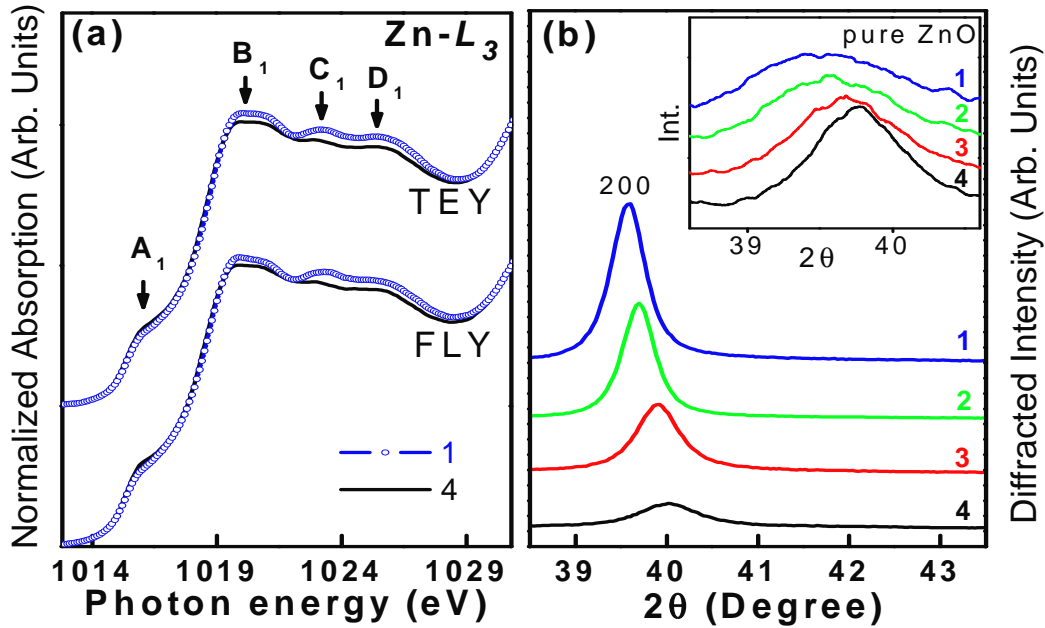


FIG. 2. (a) Bulk sensitive (FLY) and surface sensitive (TEY) Zn  $L_3$ -edge XANES spectra of the  $c$ -axis oriented AZO thin films deposited at circumferences of 0 and 30 mm from the target axis. (b) X-ray diffractograms of the  $c$ -axis oriented AZO thin films deposited at circumferences of 0, 10, 20 and 30 mm from the target axis. The inset displays the X-ray diffractograms for pure ZnO thin films deposited under the same conditions as AZO films.

Figure 1(b) plots the XRD diffractograms for the deposited AZO films. Only the (002) diffraction line could be observed. Thus, the films show a strong preferential orientation along the  $c$ -axis of the wurtzite structure, consistent with previous findings for MS-deposited transparent AZO films [17, 18]. The variation in diffracted intensity

across samples 1-4 can be attributed mainly to differences in crystal quality, as  $\omega$ -scans did not reveal significant *c*-axis tilting and the grain size estimated using the Scherrer formula [19] remained stable at  $27 \pm 3$  nm. The trend in conductivity across the samples is the opposite to that of the diffracted intensity, which suggests the dopant efficiency is reduced while the crystal quality improves. That is in contradiction with the introduction of compensating defects such as  $V_{Zn}^{''}$  or the segregation of Al in a secondary phase that degrades the crystallinity and hinders the crystal growth [20], respectively. To the contrary, undoped ZnO films deposited under the same sputtering conditions exhibit degradation of the crystal quality and a smaller average grain size as the sample is positioned closer to the magnetron axis. Such a difference highlights that the local environment of Al atoms triggers a structural reorganization in the AZO thin films. The formation of a metastable  $Al_2O_3(ZnO)_m$  homologous phase for the local environment of Al, in analogy to  $In_2O_3(ZnO)_m$  ( $m$ : integer  $\geq 3$ ) has recently been reported in pulsed laser deposited ZnO- $Al_2O_3$  supersaturated solid solutions (Al contents greater than 10 at.%) [15]. Such a phase introduces an expansion of the *c*-axis parameter when compared to bulk undoped ZnO. A progressive expansion of the *c*-axis parameter is observed in our AZO films, the value is 0.35% to 1.48% higher than that of pure bulk ZnO ( $c = 0.5205$  nm) for sample 4 and 1, respectively. The same kind of evolution is observed in undoped films deposited under the same conditions but can be linked to the increase of in-plane compressive stresses due to the bombardment by energetic oxygen ions [21]. In the AZO films presented in this study we believe that the incoming flux of energy and stress induced *c*-axis expansion trigger the formation of the metastable homologous phase. This hypothesis is fully consistent with an improvement of the

crystal quality with *c*-axis expansion as well as with a degradation of the electrical conductivity.

Figure 3 shows FLY and TEY XANES spectra of samples 1 and 4 at the *Al K* edge. According to the dipole-transition selection rule, *Al K* edge XANES probes the unoccupied *Al 3p* derived states.

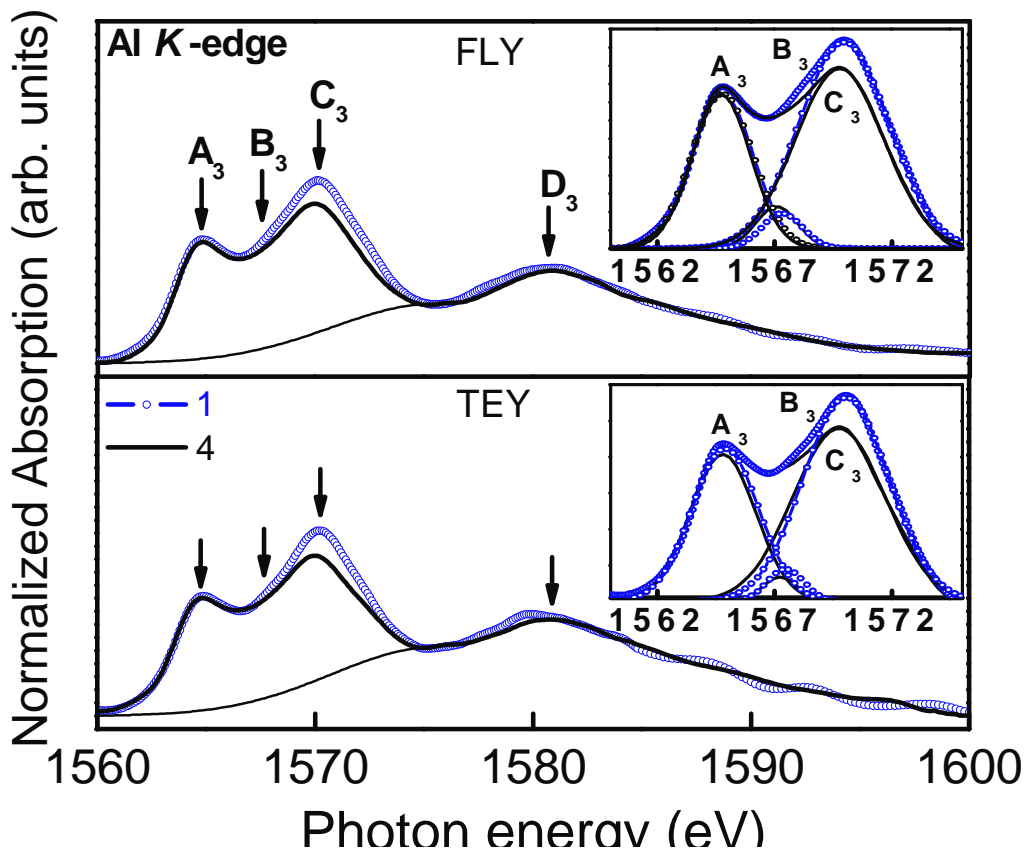


FIG. 3. Bulk sensitive (FLY) and surface sensitive (TEY) *Al K*-edge XANES spectra of *c*-axis oriented AZO thin films deposited at circumferences of 0 and 30 mm from the target axis. The insets show the magnified low energy features after background subtraction and Gaussian fitting.

Features A<sub>3</sub> (1564.6 eV), B<sub>3</sub> (1567 eV) and the broad feature D<sub>3</sub> (1581 eV) originate from *p-d* hybridization splitting of the T<sub>2</sub> orbital of Al in a tetrahedral

conformation with oxygen. Van Bokhoven *et al* [22] concluded by utilizing the extended Hückel molecular orbital (EHMO) and full multiple scattering methods that  $A_3$  is predominantly nonbonding and  $D_3$  is a local Al-O antibonding  $\sigma^*$  orbital. Feature  $C_3$  (1570 eV) is mainly ascribed to the  $T_{1u}$  level of Al in an octahedral conformation with oxygen [22]. The Al  $K$  edge spectra reveal that the intensities of features  $A_3$  and  $D_3$  are independent of the position of the sample, whereas the intensity of feature  $C_3$  is highly sensitive to the sample position. The right side insets of Figure 3 are magnified views of the  $A_3$ - $C_3$  near-edge features after subtraction of the background using a best-fit Gaussian curve;  $A_3$ - $C_3$  were deconvoluted by Gaussian fitting ( $\chi^2 =$  approx.  $10^{-4}$ ). It is clear from this analysis that a portion of the Al dopants is deactivated by its positioning in octahedral conformation with oxygen. This portion increases as the samples are placed closer to the target axis. This conformation can be found in  $Al_2O_3$  as well as in the  $Al_2O_3(ZnO)_m$  homologous phase.

These preliminary investigations verify that the partial distribution of Al into inactive (from a doping viewpoint) octahedral sites reduces the electronic conductivity of AZO films containing 4 at% Al. The combined XRD and XANES analyses suggest that these sites are likely located in  $Al_2O_3$ -like insulating nanolayers of homologous  $Al_2O_3(ZnO)_m$ , where  $m$  regulates the value of the  $c$ -axis parameter. This mechanism may be a third reason for the deactivation of the Al-dopants besides the formation of compensation Zn vacancies and precipitation of a secondary  $Al_2O_3$  phase. The proportion of Al atoms in inactive octahedral sites varies with the position relative to the target, thus explaining the lateral heterogeneity observed in moderately doped sputtered AZO films. Therefore, future efforts to develop efficient low-temperature reactively sputtered AZO based devices should avoid the distribution of Al to octahedral conformations. To achieve this, deposition techniques should be used that

not only control the composition stoichiometry of the AZO films but also minimize local electronic heterogeneities during growth. Further investigations are required to ascertain the formation of the homologous phase.

## References

- [1] Ko Park SH, Hwang CS, Jeong HY, Chu HY, Cho KI 2008 *Electrochem. Solid-State Lett.* **11** H10
- [2] Bose S and Barua AK 1999 *J. Phys. D: Appl. Phys.* **32** 213
- [3] Banerjee A and Guha S 1991 *J. Appl. Phys.* **69** 1030
- [4] Ohta H, Kawamura KI, Orita M and Hirano M 2000 *Appl. Phys. Lett.* **77** 475
- [5] Pearton SJ, Norton DP, Ip K, Heo YW and Steiner T 2005 *Progr. Mat. Sci.* **50** 293
- [6] Exharos GJ and Zhou XD 2007 *Thin Solid Films* **515** 7025
- [7] Horwat D and Billard A 2007 *Thin Solid Films* **515** 5444
- [8] Tominaga K, Kuroda K and Tada O 1988 *Jpn. J. Appl. Phys.* **27** 1176
- [9] Harding GL, Window B and Horrigan EC 1991 *Solar Energy Mater.* **22** 69
- [10] Uthanna S, Subramanyam TK, Srinivasulu Naidu B and Mahann Rao G 2002 *Opt. Mater.* **19** 461
- [11] Burstein E 1954 *Phys. Rev.* **93** 632
- [12] Zhang SB, Wei SH and Zunger A 2001 *Phys. Rev. B* **63** 075205
- [13] Butkhuzi TV, Bureyev AV, Georgobiani AN, Kekelidze NP and Khulordava TG 1992 *J. Cryst. Growth* **117** 366
- [14] Ellmer K 2000 *J. Phys. D: Appl. Phys.* **33** R17
- [15] Yiohioka S, Oba F, Huang R, Tanaka I, Mizogushi T, Yamamoto T 2008 *J. Appl. Phys.* **103** 014309

- [16] Chiou JW, Krishna Kumar KP, Jan JC, Tsai HM, Bao CW, Pong WF, Chien FZ, Tsai MH, Hong IH, Klauser R, Lee JF, Wu JJ and Liu SC 2004 *Appl. Phys. Lett.* **85** 3220
- [17] Jiang X, Jia CL and Szyszka B 2002 *Appl. Phys. Lett.* **80** 3090
- [18] Birkholz M, Selle B, Fenske F and Fuhs W 2003 *Phys. Rev. B* **68** 205414
- [19] Klug HP and Alexander LE 1974 *X-Ray Diffraction Procedures for Polycrystalline and Amorphous Materials* (Wiley, New York)
- [20] Sieber I, Wanderka N, Urban I, Dörfel I, Schierhorn E, Fenske F and Fuhs W 1998 *Thin Solid Films* **330** 108
- [21] Kaltofen R and Weise G 1993 *J. Nucl. Mater.* **200** 375
- [22] Van Bokhoven JA, Nabi T, Sambe H, Ramaker DE and Koningsberger DC 2001 *J. Phys: Condens. Matter* **13** 10247

## Figures caption

FIG. 1. Optical transmittance spectra of c-axis oriented AZO films deposited on a rotating substrate at circumferences of 0, 10, 20 and 30 mm from the target axis. The lower inset displays a schematic of the experimental configuration. The upper inset displays the dependency between the electronic conductivity and optical band gap shift.

FIG. 2. (a) Bulk sensitive (FLY) and surface sensitive (TEY) Zn  $L_3$ -edge XANES spectra of the c-axis oriented AZO thin films deposited at circumferences of 0 and 30 mm from the target axis. (b) X-ray diffractograms of the c-axis oriented AZO thin films deposited at circumferences of 0, 10, 20 and 30 mm from the target axis. The inset displays the X-ray diffractograms for pure ZnO thin films deposited under the same conditions as AZO films.

FIG. 3. Bulk sensitive (FLY) and surface sensitive (TEY) Al K-edge XANES spectra of c-axis oriented AZO thin films deposited at circumferences of 0 and 30 mm from the target axis. The insets show the magnified low energy features after background subtraction and Gaussian fitting.

